Development 134, 579-590 (2007) doi:10.1242/dev.02747

# Mammalian Polycomb Scmh1 mediates exclusion of Polycomb complexes from the XY body in the pachytene spermatocytes

**Yuki Takada[1], Kyo-ichi Isono[1], Jun Shinga[1], James M. A. Turner[2], Hiroshi Kitamura[1], Osamu Ohara[1], Gen Watanabe[3], Prim B. Singh[4], Takehiko Kamijo[5], Thomas Jenuwein[6], Paul S. Burgoyne[2] and Haruhiko Koseki[1,*]**

The product of the Scmh1 gene, a mammalian homolog of *Drosophila* Sex comb on midleg, is a constituent of the mammalian Polycomb repressive complexes 1 (Prc1). We have identified Scmh1 as an indispensable component of the Prc1. During progression through pachytene, Scmh1 was shown to be excluded from the XY body at late pachytene, together with other Prc1 components such as Phc1, Phc2, Rnf110 (Pcgf2), Bmi1 and Cbx2. We have identified the role of Scmh1 in mediating the survival of late pachytene spermatocytes. Apoptotic elimination of *Scmh1*$^{-/-}$ spermatocytes is accompanied by the preceding failure of several specific chromatin modifications at the XY body, whereas synapsis of homologous autosomes is not affected. It is therefore suggested that Scmh1 is involved in regulating the sequential changes in chromatin modifications at the XY chromatin domain of the pachytene spermatocytes. Restoration of defects in *Scmh1*$^{-/-}$ spermatocytes by *Phc2* mutation indicates that Scmh1 exerts its molecular functions via its interaction with Prc1. Therefore, for the first time, we are able to indicate a functional involvement of Prc1 during the meiotic prophase of male germ cells and a regulatory role of Scmh1 for Prc1, which involves sex chromosomes.

**KEY WORDS: Mouse, Polycomb, Scmh1, Spermatogenesis, Apoptosis, XY body**

## INTRODUCTION

The Polycomb group (PcG) genes were first identified by their requirement for the maintenance of the stable repression of Hox genes during the development of *Drosophila melanogaster* (Jürgens, 1985; Paro, 1995; Pirrotta, 1997). *Drosophila* PcG gene products form large multimeric protein complexes and are thought to act by changing the local chromatin structure, as suggested by the synergistic genetic interactions between mutant alleles of different *Drosophila* PcG genes (Jürgens, 1985; Franke et al., 1992; Paro, 1995; Pirrotta, 1997; Shao et al., 1999). In mammals, genes structurally and functionally related to *Drosophila* PcG genes have been identified and mammalian PcG gene products form several distinct complexes. Polycomb repressive complex-2 (Prc2), which contains the product of Eed (the ortholog of the *Drosophila* extra sex combs gene), Ezh2 (the ortholog of the *Drosophila* enhancer of zeste gene) and Suz12, mediates trimethylation of histone H3 at K27 (H3-K27) by Ezh2 component (Schumacher et al., 1996; Laible et al., 1997; van Lohuizen et al., 1998; Sewalt et al., 1998; van der Vlag and Otte, 1999). The second complex, which is closely related to the Polycomb repressive complex-1 (Prc1) in *Drosophila*, includes the products of the paralogs of class 2 PcG genes (Levine et al., 2002). This subset contains gene groups, namely *Pcgf2* (also known as *Rnf110* and *Mel18*, and hereafter referred to as *Rnf110*) and *Bmi1*, *Cbx2* (also known as *M33*), *Cbx4* (also known as *MPc2*) and *Cbx8* (also known as *Pc3*), *Phc1* (also known as *rae28*), *Phc2* and *Phc3*, *Ring1* and *Rnf2* (also known as *Ring1B*) (Levine et al., 2002). The Prc1 complex is compositionally and functionally conserved between flies and mammals (Shao et al., 1999; Levine et al., 2002; Gebuhr et al., 2000). In mammals, chromatin binding of Prc1 involves its recognition of trimethylated H3-K27 (Boyer et al., 2006; Lee et al., 2006; Fujimura et al., 2006). The Prc1 complex has a significant impact on the control of not only anteroposterior (AP) specification of the axis via Hox regulation, but also the proliferation and senescence via regulation of the Ink4a/p53 pathway (Jacobs et al., 1999).

*Sex comb on midleg* (*Scm*) gene is a member of *Drosophila PcG* genes and, based on database comparison, its product contains three separable functional domains (Bornemann et al., 1996), namely: a pair of N-terminal zinc fingers, two tandem 100-amino acid repeats, called mbt repeats as they are also found in the fly tumor suppressor encoded by the *l(3)mbt* [*lethal(3) malignant brain tumor*] gene, and C-terminal homology domain of 65 amino acids, called the SPM domain. The SPM domain is a self-binding protein interaction module and may mediate Scm association to Prc1 and play a key role for PcG repression, although Scm association to purified Prc1 is substoichiometric (Levine et al., 2002). In mammals, there are four paralogs for *Drosophila Scm* based on primary sequence: *Scmh1*, *Scml1*, *Scml2* and *Sfmbt* (Tomotsune et al., 1999; van de Vosse et al., 1998; Montini et al., 1999; Usui et al., 2000). The mammalian Scmh1 protein has been shown to be a constituent of the mammalian Prc1 (Levine et al., 2002), which contains two highly conserved motifs, two mbt repeats in the N-terminal region and an SPM domain in the C-terminal region, that are shared with its *Drosophila* counterpart. The SPM domain of Scmh1 can mediate its

[1]RIKEN Research Center for Allergy and Immunology, 1-7-22 Suehiro, Tsurumi-ku, Yokohama 230-0045, Japan. [2]Division of Stem Cell Research and Developmental Genetics, MRC National Institute for Medical Research, The Ridgeway, Mill Hill, London NW7 1AA, UK. [3]Laboratory of Veterinary Physiology, Tokyo University of Agriculture and Technology, Fuchu, Tokyo 183-8509, Japan. [4]Nuclear Reprogramming Laboratory, Division of Gene Expression and Development, Roslin Institute (Edinburgh), Roslin, Midlothian EH25 9PS, UK. [5]Department of Pediatrics, Shinshu University School of Medicine, Matsumoto, Nagano 390-8621, Japan. [6]Research Institute of Molecular Pathology, The Vienna Biocenter, Dr Bohrgasse 7, A-1030 Vienna, Austria.

*Author for correspondence (e-mail: koseki@rcai.riken.jp)

**Accepted 17 November 2006**

interaction with *Drosophila* polyhomeotic (Ph) and mammalian Phc1 and Phc2, through their respective SPM domains (Tomotsune et al., 1999). It is also notable that tissue-specific *Scmh1* mRNA levels in the testes are the highest of all tissues analyzed and they increase during the synchronous progression of first-wave spermatogenesis in parallel with *Phc1* (see Fig. S1A,B in the supplementary material). These observations suggest a role of mammalian Prc1 during spermatogenesis.

Before the specialized cell division of meiosis, postmitotic spermatocytes enter into an extended meiotic prophase, in which homologous autosomal chromosomes pair and undergo reciprocal recombination. There is accumulating evidence to suggest that the quality of this complex process is monitored by a checkpoint to ensure spermatogenic success, as represented by the apoptotic elimination of those spermatocytes with synaptic errors. During this period, heteromorphic sex chromosomes pair only in a small pseudoautosomal region (PAR) at their distal ends and undergo transcriptional inactivation, termed meiotic sex chromosome inactivation (MSCI), by remodeling into heterochromatin, thus forming the XY body (Perry et al., 2001; Odorisio et al., 1996; Singer-Sam et al., 1990; Turner et al., 2004; Baarends et al., 1999; Strahl and Allis, 2000; Turner et al., 2000; Hoyer-Fender et al., 2000; Mahadevaiah et al., 2001; Khalil et al., 2004). Formation of the XY body is conserved throughout the mammalian phylogenetic tree and is therefore assumed to be essential for successful spermatogenesis and the faithful segregation of sex chromosomes. Indeed, in mutants for the gene encoding histone H2A.X and the tumor suppressor protein Brca1, failure to form the XY body coincides with sterility due to the apoptotic elimination of such mutant spermatocytes before completion of meiosis (Fernandez-Capetillo et al., 2003; Xu et al., 2003). However, it has not been definitely demonstrated that spermatogenic arrest in these mutants is because of failure to form the XY body or due to some other reason. The condensation of the X and Y chromosome to form the XY body is associated with post-translational modifications of histones and the recruitment or exclusion of various chromatin-associated proteins (Turner et al., 2001; Hoyer-Fender et al., 2000; Richler et al., 2000; Mahadevaiah et al., 2001; Khalil et al., 2004; Baarends et al., 1999; Baarends et al., 2005). Early in the formation of the XY body, phosphorylated histone H2A.X (γH2A.X) and ubiquitylated histone H2A (uH2A) are enriched at the XY body and then X and Y chromosomes undergo sequential changes in their histone modifications, which correlate with transcriptional status of sex chromosomes (Mahadevaiah et al., 2001; Baarends et al., 1999; Baarends et al., 2005). The functional involvement of these histone modifications at the XY body was properly addressed for the first time in a study using *Brca1* mutants, in which H2A.X phosphorylation was shown to be essential to trigger MSCI (Turner et al., 2004). However, the roles of hyperubiquitylation of H2A on the X and Y chromosomes have still not been addressed. Recent studies have revealed an Rnf2 component of Prc1 to be an E3 component of ubiquitin ligase for histone H2A to link Prc1 with the XY body (de Napoles et al., 2004; Baarends et al., 1999; Baarends et al., 2005).

In this study, we have generated a mouse line carrying a mutant *Scmh1* allele that lacks the exons to encode an SPM domain. Axial homeotic transformations and premature senescence in mouse embryonic fibroblasts (MEFs) in the homozygotes indicated the role of Scmh1 as a PcG component. Approximately half the *Scmh1*$^{-/-}$ males were infertile, which correlates with an accelerated apoptosis of postmitotic pachytene spermatocytes. The present genetic study indicates the involvement of Prc1 during XY body maturation and the regulatory role of Scmh1 gene products in the exclusion of Prc1 from the XY body, which may in turn be required for the further progression of meiotic prophase.

## MATERIALS AND METHODS

### Mice

*Scmh1*-deficient mice were generated using R1 embryonic stem (ES) cells according to the conventional protocol and backcrossed to C57BL/6 background four to six times (Akasaka et al., 1996). Schematic representations of genomic organization and targeting vector are shown in Fig. S2 in the supplementary material. *Scmh1* mutant mice were genotyped by PCR using the following oligonucleotides: (a) 5′-GTCAG-GTGTGCCCGCTACTGT-3′ and (b) 5′-GATGGATTGCACGCAGGTTC-3′ for the mutant allele; and (a) and (c) 5′-GGCCGACTAGGC-CATCTTCTG-3′ for the *Scmh1* wild-type allele. As *Scmh1* and *Phc2* loci were on chromosome 4 and $28\times10^6$ base pairs (bp) apart from each other, we first generated recombinants in which *Scmh1* and *Phc2* mutant alleles were physically linked. This double mutant allele was used to generate *Scmh1;Phc2* double homozygotes. Skeletal analysis was performed as described previously (Kessel and Gruss, 1991). MEFs were maintained according to a 3T9 protocol as described previously (Kamijo et al., 1997).

### In situ hybridization, RT-PCR and immunohistochemistry

In situ hybridization was performed as described previously (Yuasa et al., 1996). The nucleotide sequences of the primers used for RT-PCR in this study are listed in Table 1. Immunohistochemistry was performed as described previously (Hoyer-Fender et al., 2000).

### TUNEL staining

Apoptotic cells were visualized by the terminal deoxynucleotidetransferase-mediated dUTP nick end-labeling (TUNEL) assay (In Situ Cell Death Detection Kit, AP; Roche, Germany).

### Immunocytochemistry of spread spermatocytes

Meiotic prophase cell spreads and squashes were prepared as described previously (Scherthan et al., 2000). After washing with PBS for 3 minutes, slides bearing cell spreads were processed for immunostaining using standard procedures. The antibodies used for immunostaining in this study are listed in Table 2. For the statistical analyses, 300 spermatocytes derived from five mice with respective genotypes were analyzed and the significance was further analyzed by *t*-test.

### Microarray analysis

Microarray analysis was performed using Mouse Genome 430 2.0 GeneChips (Affymetrix, Santa Clara, CA) according to the manufacturer's instructions. The intensity for each probe set was calculated using the MAS5 method of the GCOS software package (Affymetrix) at the default setting. Per chip normalization was performed using a median correction program in the GeneSpring software package (Agilent Technologies, Palo Alto, CA). One comparison between the two groups was conducted using a triplicate array. Data of probe sets were excluded from the analyses when they were judged to be 'absent' by the GCOS program in at least one sample in the stimulated groups. Probe sets that differentially hybridized between the samples were identified by the following criteria: (1) Welch's analysis of variance (ANOVA) showed that the *P*-value was less than 0.05; (2) the Benjamini and Hochberg false discovery test confirmed the ANOVA result; and (3) more than a twofold difference in the expression levels was observed between the samples.

## RESULTS

### Scmh1 is a functional component of PcG complexes

We generated a mutant allele for Scmh1 by deleting the sequences encoding the SPM domain, in which a small amount of truncated *Scmh1* transcript was expressed (see Fig. S2A-E in the supplementary material). As the *Drosophila Scm*$^{XF24}$ allele, in which the SPM domain is exclusively affected, presents an almost identical phenotype to null alleles, the *Scmh1* mutant allele could be a null or

**Table 1. Primers used in semiquantitative RT-PCR analyses**

| Gene | Forward (5′→3′) | Reverse (5′→3′) |
|---|---|---|
| *A-myb* | aagaagttggttgaacaacacgg | aggaagtaacttagcaatctcgg |
| *Dmc1* | ttcgtactggaaaaactcagctgtatc | cttggctgcgacataatcaagtagctcc |
| *Mvh1* | ccaaaagtgacatatataccc | ttggttgatcacttctcgag |
| *Scp-3* | ggtggaagaaagcattctgg | cagctccaaatttttccagc |
| *CyclinA1* | atgcatcgccagagctccaagag | ggaagtggagatctgacttgagc |
| *Calmegin* | atatgcgtttccagggtgttggac | gtatgcacctccacaatcaatacc |
| *Bmp8a* | ggctcgagatggtggtcaaggcctgtgg | ggggatccaggctctttctatgtggcc |
| *CREMτ* | gattgaagaagaaaaatcaga | catgctgtaatcagttcatag |
| *β-actin* | gagagggaaatcgtgcgtga | acatctgctggaaggtggac |
| *Scmh1* | | |
| Primers 1/2 | atgctggtttgctac | aggacaaaggtttcacct |
| Primers 3/4 | actgccacagagtataatca | tcagaacttgccctg |

**Table 2. Antibodies used in immunostaining analyses**

| Antibody | Species | Dilution | Company |
|---|---|---|---|
| Anti-p53(clone pAb421) | Rabbit | 1:500 | Oncogene Research Products |
| Anti-Scp3 | Rabbit | 1:100 | Novus Biologicals |
| Anti-phospho-H2A.X (Ser139) | Rabbit | 1:500 | Upstate |
| Anti-ubiquityl-Histone H2A(clone E6C5) | Mouse | 1:100 | Upstate |
| Anti-monomethyl-Histone H3(Lys9) | Rabbit | 1:100 | Upstate |
| Anti-dimethyl-Histone H3(Lys9) | Rabbit | 1:100 | Upstate |
| Anti-acetyl-Histone H3 | Rabbit | 1:100 | Upstate |
| Anti-trimethyl-Histone H3 (Lys27) | Rabbit | 1:100 | Upstate |
| Anti-dimethyl-Histone H4 (Lys20) | Rabbit | 1:100 | Upstate |
| Anti-monomethyl-Histone H3 (Lys4) | Rabbit | 1:100 | Upstate |
| Anti-Rad51 (H-92) | Rabbit | 1:50 | Santa Cruz |
| Anti-Mlh1 (G168-15) | Mouse | 1:50 | BD Pharmingen |
| Anti-phosphorylated RNA polymerase II | Mouse | 1:25 | Covance |
| Anti-Scmh1 | Mouse | Undiluted | This study |
| Anti-Phc1 | Mouse | Undiluted | Miyagishima et al., 2003 |
| Anti-Phc2 | Mouse | Undiluted | Isono et al., 2005 |
| Anti-Bmi1(H-99) | Rabbit | 1:25 | Santa Cruz |
| Anti-Rnf110(C-20) | Rabbit | 1:30 | Santa Cruz |
| Anti-Cbx2(C-18) | Rabbit | 1:25 | Santa Cruz |
| Anti-Rnf2 | Mouse | Undiluted | Atsuta et al., 2001 |
| Anti-Ezh2 | Rabbit | 1:100 | Upstate |
| Anti-mouse IgM FITC | Donkey | 1:100 | Becton Dickinson |
| Anti-mouse IgG Cy2 | Donkey | 1:100 | Jackson ImmunoResearch Laboratories |
| Anti-rabbit IgG Cy3 | Donkey | 1:500 | Jackson ImmunoResearch Laboratories |
| Anti-mouse IgG (H+L) Alexa Fluor 488 | Goat | 1:300 | Molecular Probes |
| Anti-rabbit IgG (H+L) Alexa Fluor 568 | Goat | 1:300 | Molecular Probes |
| Anti-rabbit IgG, HRP-conjugated | Goat | 1:2000 | Amersham |

strong hypomorphic mutation (Bornemann et al., 1996). Although both male and female *Scmh1*$^{-/-}$ mice were viable and grew normally to adulthood, homozygotes exhibited the axial homeosis and premature senescence of MEFs in the homozygous mutants, which was restored by the *p19*$^{ARF}$ or *p53* mutation (see Fig. S2F-K in the supplementary material). Therefore, Scmh1 is an indispensable component of Prc1 in mice.

## The expression and subcellular localization of Scmh1 during spermatogenesis

About half the homozygotes were sterile and had slightly smaller testes than their wild-type littermates (Y.T., unpublished). Before studying the pathogenesis of infertility in *Scmh1* mutants, we examined Scmh1 expression during spermatogenesis by in situ hybridization and immunohistochemical analysis. *Scmh1* expression was seen in the seminiferous tubules and interstitial cells (Fig. 1Aa). In the seminiferous tubules, morphological examination of the germ cell layers representing meiotic spermatocytes (particularly those at the pachytene stage) revealed that these germ layers were expressing the highest amount of *Scmh1*, with the least amounts expressed in spermatogonia and round spermatids (Fig. 1Ab). Sertoli cells also expressed a significant amount of *Scmh1*. By using an immunohistochemical technique, a light staining of the whole nucleus was observed in the zygotene stage and in more advanced cells up to pachytene spermatocytes (Fig. 1Ba). In addition, focal localization of Scmh1 was seen in the chromocenter of round spermatids (Fig. 1Bb). Concordantly, *Scmh1* expression in the testes correlated with synchronous progression of the first-wave spermatogenesis (see Fig. S1B in the supplementary material). From day 15 post partum (pp) onwards, the amount of *Scmh1* transcript progressively increased and reached a maximum level by day 25 pp. Taken together, *Scmh1* and its products are predominantly expressed in postmitotic spermatocytes.

We went on to investigate subcellular localization of Scmh1 by using spread meiotic spermatocytes. The synaptonemal complex protein Scp3, which is a component of the axial element, was used to substage meiosis (Xu et al., 2003). Scmh1 staining was seen in the nucleus as a diffused pattern from leptotene to early pachytene spermatocytes (Fig. 1Ca-c and Y.T., unpublished). In late pachytene spermatocytes, Scmh1 staining was significantly excluded from the

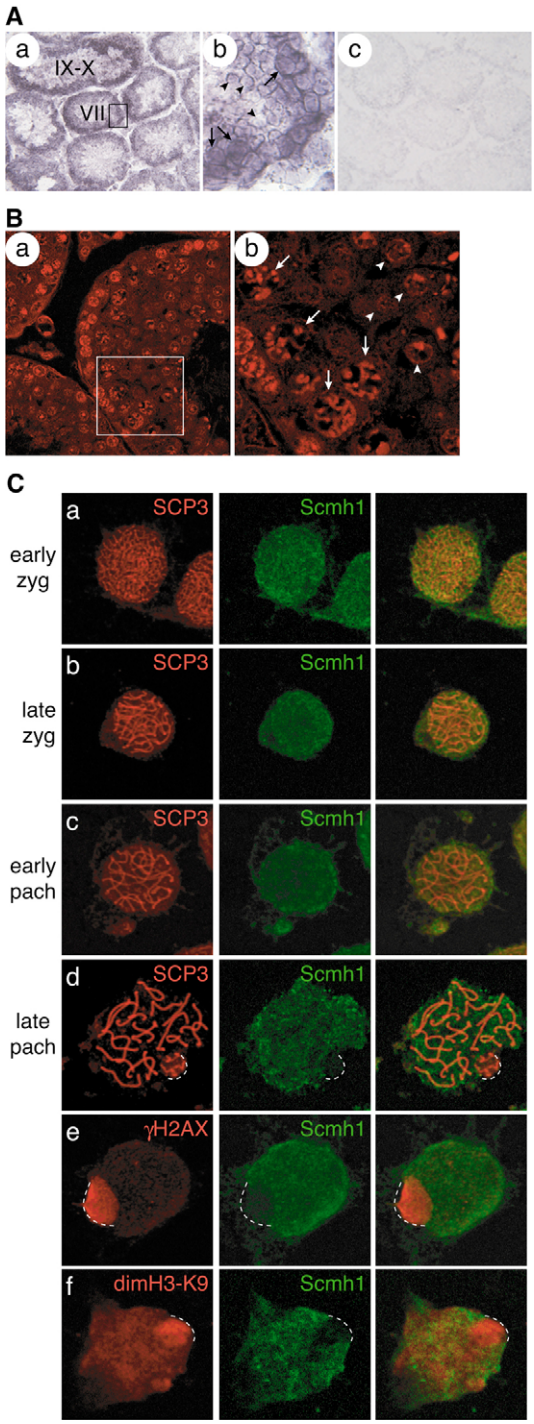


**Fig. 1. Localization of Scmh1 in the adult testes and spermatocytes.** (**Aa**) In situ hybridization using antisense probe. Stages of seminiferous tubules are given. (**Ab**) Higher magnification view of seminiferous tubule at stage VII shown in a. Arrows and arrowheads indicate pachytene spermatocytes and round spermatids, respectively. (**Ac**) Control slides using sense probe. (**Ba**) Immunohistochemical localization of Scmh1 of wild-type testes. (**Bb**) Higher magnification view of seminiferous tubule shown in a. Arrows and arrowheads indicate pachytene spermatocytes and round spermatids, respectively. (**C**) Immunocytochemical detection of Scmh1 gene products from zygotene to pachytene stage spermatocytes, which were prepared from day 18 pp wild-type testes. (**Ca-Cd**) Spermatocyte spreads were substaged into early (a) and late (b) zygotene and early (c) and late (d) pachytene stages based on anti-Scp3 (red) immunostaining and morphology. Scmh1 (green) was localized in the nuclei at each stage, but was mostly excluded from the X and Y chromosome territory at late pachytene stage, as indicated by dotted lines. (**Ce**) Reciprocal subnuclear localization of Scmh1 and γH2A.X indicated exclusion of Scmh1 from the XY body. The XY body is indicated by dotted lines. (**Cf**) Reciprocal subnuclear localization of Scmh1 and dimethylated H3-K9 indicated exclusion of Scmh1 from the XY body. The XY body is indicated by dotted lines.

XY chromatin domain (Fig. 1Cd,e). Concordantly, reciprocal localization of Scmh1 and γH2A.X was seen in about 80% of pachytene spermatocytes (Fig. 1Ce). Consistently, Scmh1 was excluded from the XY body in which dimethylated histone H3 at K9 (H3-K9) was enriched (Fig. 1Cf).

## Subcellular localization of PcG proteins and trimethylated H3-K27 during spermatogenesis

The progressive exclusion of Scmh1 from the XY body during the pachytene stage prompted us to examine the subcellular localization of other PcG proteins and trimethylated H3-K27, which is mediated by the Ezh2 component of Prc2. Subcellular localization of Phc1, Phc2, Bmi1, Rnf110 and Cbx2 were compared with γH2A.X or uH2A. Reciprocal localization of these PcG proteins and γH2A.X or uH2A, within about 80% of spermatocytes, indicated the exclusion of other PcG proteins from the XY body during the pachytene stage, as well as Scmh1 (Fig. 2Aa-e). Consistently, Phc2 was excluded from the XY body in 77% of spermatocytes, in which dimethylated H3-K9 was enriched (Fig. 2Af). Taken together, PcG complexes are excluded from the XY body at the late pachytene stage almost concurrently with hyperdimethylation of H3-K9 at the XY body, whereas they are continuously present in the autosomal regions.

Recent studies have repeatedly provided evidence indicating the engagement of Prc1 by trimethylated H3-K27 mediated by Prc2 (Cao et al., 2002; Kuzmichev et al., 2002). We thus addressed whether the exclusion of Prc1 components from the XY body was correlated with the degree of H3-K27 trimethylation at the XY chromatin domain. Trimethylated H3-K27 was distributed throughout the nucleus as a diffuse pattern from leptotene to zygotene stage spermatocytes despite the fact that the signals were very dim (Fig. 2Ba and Y.T., unpublished). In early pachytene spermatocytes, trimethylated H3-K27 staining was much stronger than in the earlier stages but was significantly excluded from the XY chromatin domain (Fig. 2Bb). In late pachytene spermatocytes, its exclusion from the XY body was still maintained (Fig. 2Bc). Therefore the exclusion of trimethylated H3-K27 from the XY chromatin domain precedes those of Prc1 components.

## Impaired spermatogenesis in *Scmh1*$^{-/-}$ males

We first examined the histology of *Scmh1*$^{-/-}$ testes in day 35 pp testes and revealed that about two-thirds were morphologically altered to varying extents. The seminiferous tubules of *Scmh1*$^{-/-}$ testes exhibited a reduction in the number of spermatocytes and a lack of spermatids and mature spermatozoa (Fig. 3Aa,b). Sertoli cells and spermatogonia were morphologically and numerically normal. Mono- or multinuclear large cells were sometimes seen. One-third of *Scmh1*$^{-/-}$ testes were morphologically indistinguishable from wild type. Therefore, spermatogenesis was variably affected in *Scmh1*$^{-/-}$ testes.

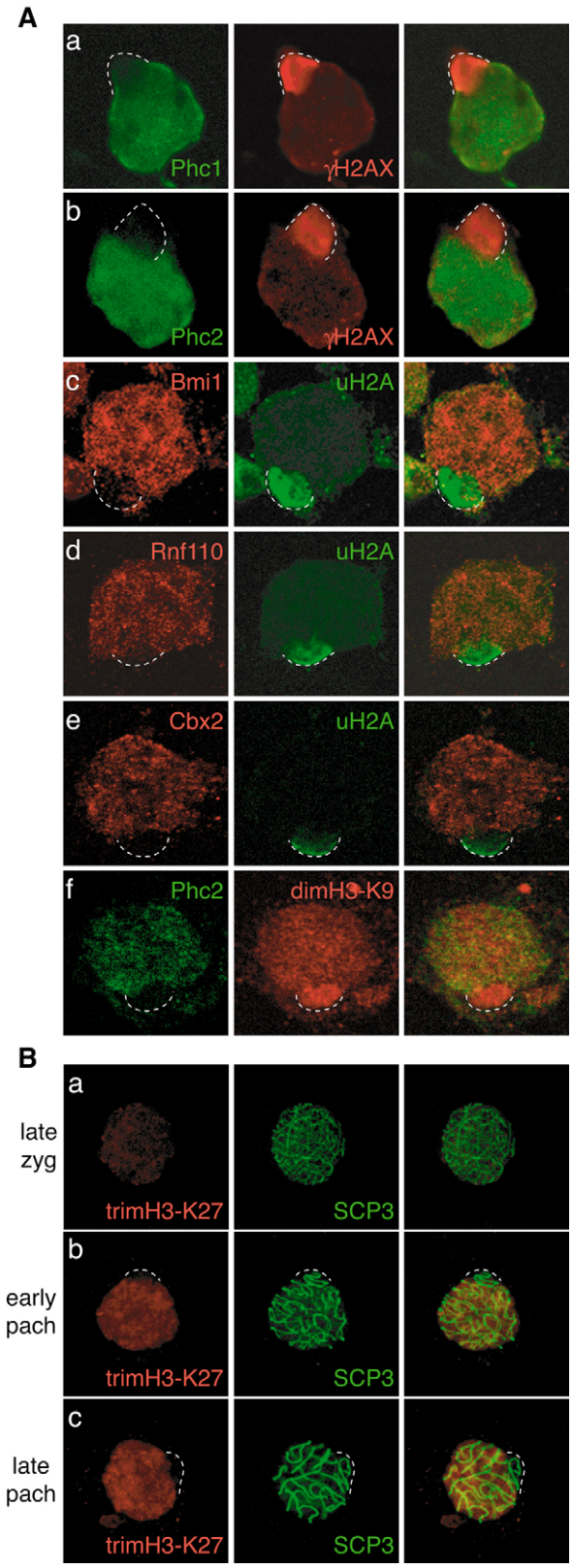


**Fig. 2. Expression pattern of other PcG proteins and trimethylated H3-K27 at pachytene stage spermatocytes.** (**A**) Immunocytochemical detection of Prc1 components in pachytene spermatocytes. (**Aa**,**Ab**) Phc1 (a) and Phc2 (b) were excluded from the XY body demarcated by extensive accumulation of γH2A.X. (**Ac-Ae**) Bmi1 (c), Rnf110 (d) and Cbx2 (e) were excluded from the XY body demarcated by extensive accumulation of uH2A. The XY body is indicated by dotted lines. (**Af**) Reciprocal subnuclear localization of Phc2 and dimethylated H3-K9 indicated exclusion of Scmh1 from the XY body. (**B**) Immunocytochemical detection of trimethylated H3-K27 from late zygotene to pachytene stage spermatocytes. Spermatocytes were immunostained by using anti-trimethylated H3-K27 (red) and anti-SCP3 (green). The X and Y chromosome territory is indicated by dotted lines.

We then examined *Scmh1*$^{-/-}$ testicular histology at various stages of first-wave spermatogenesis. Neither day 7 pp nor day 11 pp mutant mice exhibited any significant differences compared to wild type (Fig. 3B). The morphological changes in *Scmh1*$^{-/-}$ testes were observed in the seminiferous tubules as early as day 15 pp. At day 15 pp, most of the seminiferous tubules contained spermatogonia, Sertoli cells and several degenerating pachytene spermatocytes, whereas pre-leptotene to zygotene spermatocytes were seen rarely (see Fig. S3 in the supplementary material). Vacuoles were frequently seen in the luminal region. Based on these morphological parameters, days 15, 19, 25 and 30 pp testes were also examined. In conclusion, *Scmh1*$^{-/-}$ testes were progressively affected during first-wave spermatogenesis (Fig. 3B).

We went on to investigate the frequency of apoptosis during the progression of spermatogenesis by TUNEL labeling. In wild-type day 15 and 19 pp testes, a few TUNEL-labeled cells were clearly present but were seen only rarely in day 7 pp (Fig. 3Ca-c). In *Scmh1*$^{-/-}$ testes, a significant number of TUNEL-labeled cells were observed in the inner layers of seminiferous tubules at day 15 and 19 pp, but not at day 7 pp (Fig. 3Cd-h). These histological observations confirmed that postmitotic spermatocytes in meiotic prophase were predominantly affected in *Scmh1*$^{-/-}$ testes.

Finally, the expression of stage-specific molecular markers were examined by means of semi-quantitative RT-PCR analysis in wild-type and *Scmh1*$^{-/-}$ testes at day 35 pp, in order to address which stage of spermatogenesis was predominantly deleted in affected homozygous mutants (Fig. 3D). *CyclinA1*, *calmegin*, *Bmp8a* and *CREMτ* genes were used as markers for pachytene stage spermatocytes (Sweeney et al., 1996; Watanabe et al., 1994; Zhao and Hogan, 1996; Foulkes et al., 1992). These were reduced more than threefold in *Scmh1*$^{-/-}$ when compared with testes from wild type. In *Scmh1*$^{-/-}$ testes no change was observed in the expression of *A-myb*, *Dmc1*, *Mvh1* and *Scp3*, which are expressed before the pachytene stage (Mettus et al., 1994; Habu et al., 1996; Fujiwara et al., 1994; Tanaka et al., 2000; Klink et al., 1997). Taken together, in *Scmh1*$^{-/-}$ testes, postmitotic spermatocytes are predominantly depleted by apoptotic outbursts.

## Apoptotic elimination of late pachytene spermatocytes occurs after synapsis of homologous chromosomes in *Scmh1*$^{-/-}$ testes

In order to further identify the meiotic substage at which *Scmh1*$^{-/-}$ spermatocytes are predominantly affected, immunolocalization studies were carried out in spread spermatogenic cells, prepared from day 18 pp males, by using antibodies against uH2A, γH2A.X and Scp3. Accumulation of uH2A on the XY body was seen in pachytene spermatocytes, whereas γH2A.X demarcates the XY body from late zygotene to diplotene stage (Baarends et al., 1999; Baarends et al., 2005; Mahadevaiah et al., 2001; Fernandez-

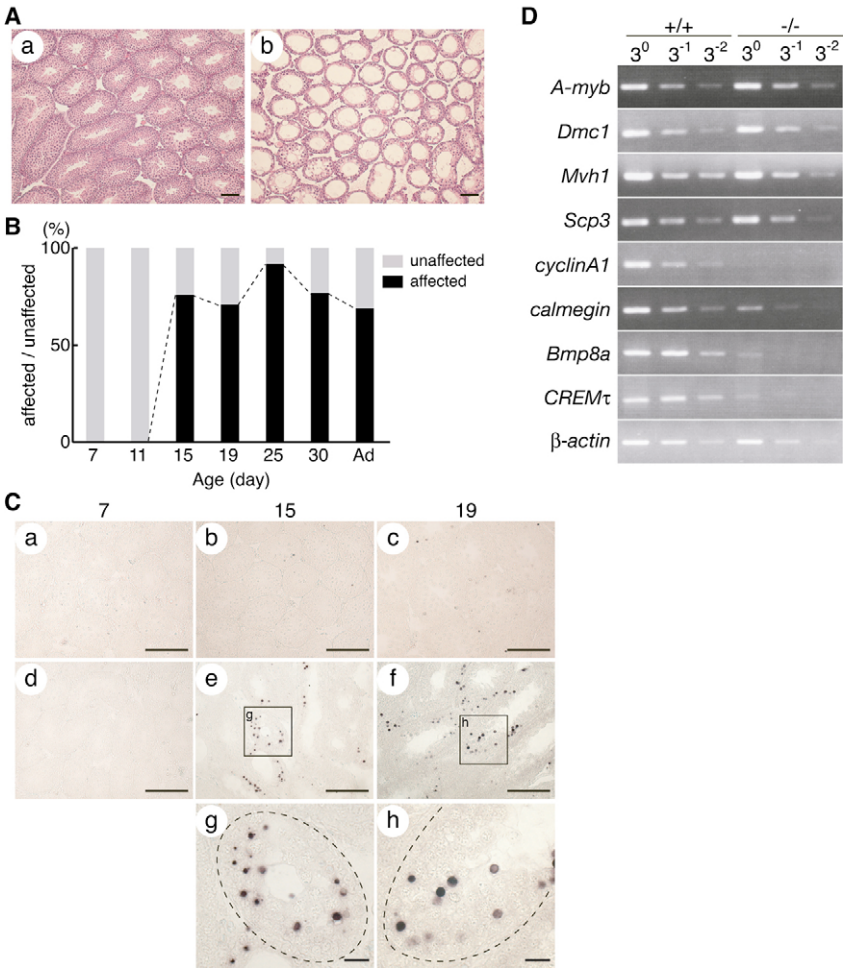


**Fig. 3. Testicular abnormalities in *Scmh1*$^{-/-}$ mice.** (**A**) Cross-sections of testes from day 35 pp wild-type (**Aa**) and *Scmh1*$^{-/-}$ (**Ab**) mice. Sections were stained with Hematoxylin and Eosin (HE). (**B**) The frequency of *Scmh1*$^{-/-}$ mice in which seminiferous tubules were morphologically affected during first-wave spermatogenesis. Days after birth are shown. At each age, more than ten mutants were examined. Mutants over 8 weeks of age were collected and indicated as adults (Ad). (**C**) Increased apoptotic spermatocytes in *Scmh1*$^{-/-}$ testes. (**Ca-Cc**) Incidence of apoptosis in wild-type testes at day 7, 15 and 19 pp. (**Cd-Cf**) Incidence of apoptosis in *Scmh1*$^{-/-}$ testes at day 7, 15 and 19 pp. (**Cg**,**Ch**) Higher magnification views of individual seminiferous tubules shown in e and f. Outline of seminiferous tubules are indicated by dotted lines. (**D**) The expression of stage-specific markers during spermatogenesis in wild-type and unaffected and affected *Scmh1*$^{-/-}$ testes at day 35 pp, as revealed by semi-quantitative RT-PCR. *β-actin* was used as a standard to verify the equal amounts of cDNA. Primers used in each reaction are shown in Table 1. Scale bars: 100 μm in A,B,Ca-Cf; 10 μm in Cg,Ch.

Capetillo et al., 2003; Xu et al., 2003). In particular, the degree of uH2A association to the XY body was intriguing, as the Rnf2 component of class 2 PcG has been shown to be an E3 component of ubiquitin ligase for histone H2A (Wang et al., 2004; de Napoles et al., 2004). We did not see any significant difference between *Scmh1*$^{-/-}$ and wild-type testes in the frequency of the spermatocytes, in which uH2A and γH2A.X localized on the XY bodies. This implies entry into pachytene stage was not affected in *Scmh1*$^{-/-}$ (Y.T., unpublished). Using Scp3 staining and morphology, we substaged further the spermatocytes, in which uH2A was accumulated on the XY body, into early and late pachytene stages (Fig. 4A). The frequency of early pachytene spermatocytes was 37% in wild type and 66% in *Scmh1*$^{-/-}$ (Fig. 4A). This suggests that *Scmh1*$^{-/-}$ spermatocytes were incompletely depleted by late pachytene.

During meiosis, synapsis is essential for proper chromosome segregation, and is monitored by various meiotic checkpoints (Cohen and Pollard, 2001). As proper chromosome alignment and segregation in the first meiotic division are ensured by recombination between homologous chromosomes, we examined the localization of Mlh1, a mismatch-repair protein, that forms foci at sites of meiotic crossover in mid- to late-pachytene spermatocytes (Celeste et al., 2002). Mlh1 foci were distributed on the synaptonemal complexes in late pachytene spermatocytes of both wild type and *Scmh1*$^{-/-}$ (Fig. 4B). Consistent with this observation, late pachytene spermatocytes remained in *Scmh1*$^{-/-}$ testes exhibited normal Scp3 distribution, including PAR of sex chromosomes (see Fig. S4 in the supplementary material). Taken together, Scmh1 is dispensable for pairing and synapsis of homologous chromosomes.

## The role of Scmh1 at the XY body in pachytene spermatocytes

Apart from homologous autosomes, the X and Y chromosomes pair along PAR and undergo extensive and sequential remodeling into heterochromatin, thus forming the XY body, which is associated with transcriptional inactivation. Failure to form the XY body has been shown to coincide with male sterility and arrest of spermatogenesis, although it is not yet definitely proven whether the XY body is required for survival and fertility of male germ cells (Fernandez-Capetillo et al., 2003). Scmh1 and other PcG components were excluded at the transition from early to late pachytene stage. *Scmh1*$^{-/-}$ spermatocytes were affected at a stage that was temporally similar to that concerning the exclusion of PcG proteins from the XY chromatin domain. These observations prompted us to focus on whether spermatogenic arrest in *Scmh1*$^{-/-}$ testes is accompanied by changes in chromatin remodeling at the XY body. We first examined the degree of H3-K9 methylation, acetylation and phosphorylated RNA pol II association to the XY bodies, which have been shown to change during the pachytene stage (Richler et al., 2000; Khalil et al., 2004). In wild type, 76 and 62% of the XY body marked by uH2A were hyperdi- and hypermonomethylated at H3-K9, respectively, compared with 36 and 18%, respectively, in *Scmh1*$^{-/-}$ testes (Fig. 5Aa,b).

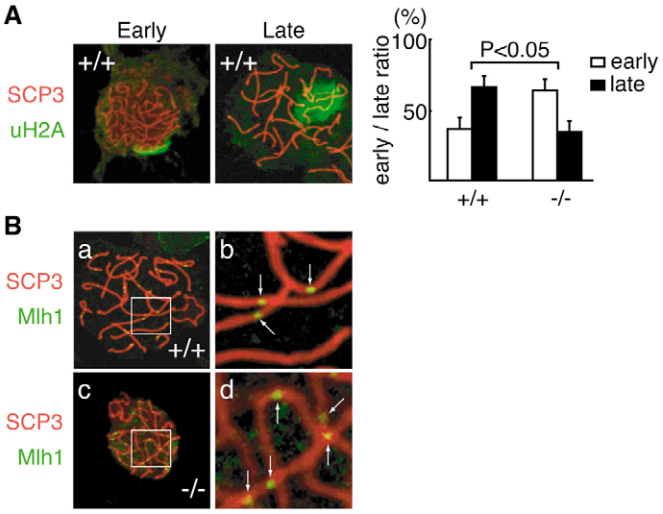


**Fig. 4. Significant reduction of late pachytene spermatocytes in *Scmh1*$^{-/-}$ testes.** (**A**) Reduction of late pachytene spermatocytes in spermatocyte spread prepared from day 18 pp *Scmh1*$^{-/-}$ testes in comparison with wild type. Spermatocytes were immunostained using anti-Scp3 (red) and uH2A (green). (Left) Wild-type spermatocytes, in which uH2A is enriched at the XY body, were examined at early or late pachytene stage, based on Scp3 immunostaining and morphology. (Right) Frequency of early and late pachytene spermatocytes was compared between the wild-type and *Scmh1*$^{-/-}$ testes. (**B**) Localization of Mlh1 in spermatocytes. (**Ba**) Spermatocytes of wild type were immunostained by using anti-Scp3 (red) and Mlh1 (green). (**Bb**) Higher magnification view of chromosomes shown in a. (**Bc**) Localization of Mlh1 in *Scmh1*$^{-/-}$ mutant testes. (**Bd**) Higher magnification view of chromosomes shown in c. Arrows in b and d indicate Mlh1 foci.

Phosphorylated RNA pol II was excluded from the XY body in 51% of the *Scmh1*$^{-/-}$ spermatocytes compared with 90% of wild type (Fig. 5Ac) (Richler et al., 2000; Khalil et al., 2004). These results suggest that elimination of late pachytene spermatocytes in *Scmh1*$^{-/-}$ testes is coincidental with the stage at which the XY body undergoes chromatin remodeling. It is also noteworthy that underacetylation of H3-K9 at the XY body was observed to a similar extent between the wild-type and *Scmh1*$^{-/-}$ spermatocytes (Fig. 5Ad). Changes in such specific chromatin modifications at the XY body of *Scmh1*$^{-/-}$ spermatocytes imply that they may not solely represent their developmental arrest at late pachytene stage. We therefore postulated a regulatory role for Scmh1 in sequential chromatin modifications of the XY body.

To address this possibility, we extended the analyses to other epigenetic modifications, which could potentially be influenced by *Scmh1* mutation. We first examined the localization of PRC1 components and trimethylated H3-K27, which was bound by PRC1, in *Scmh1*$^{-/-}$ testes. The frequency of meiotic spermatocytes exhibiting reciprocal localization of Phc1 or Phc2 and γH2A.X in *Scmh1*$^{-/-}$ spermatocytes was examined. In 79% of wild-type spermatocytes, Phc1 and Phc2 were excluded from the XY body demarcated by γH2A.X (Fig. 5Ba,b). In *Scmh1*$^{-/-}$ spermatocytes, the frequency of spermatocytes in which Phc1 and Phc2 were excluded from the XY body was reduced to 40 and 27%, respectively (Fig. 5Ba,b). Similarly, trimethylated H3-K27 was excluded from the XY body demarcated by uH2A in 88% of wild-type spermatocytes compared with 39% in *Scmh1*$^{-/-}$ spermatocytes (Fig. 5Bc). Therefore meiotic spermatocytes, in which the sequential exclusion of trimethylated H3-K27 and Prc1 components from the XY body had failed, may be predominantly depleted in *Scmh1*$^{-/-}$ testes. As the exclusion of trimethylated H3-K27 from the XY body is shown to precede the exclusion of PRC1 components in wild type, this result could be interpreted as recurrence of H3-K27 trimethylation in the late pachytene stage. We therefore substaged the spermatocytes in which trimethylated H3-K27 was excluded from the XY body into early and late pachytene stages by using Scp3 staining and morphology. In early pachytene stage, trimethylated H3-K27 was excluded from the XY body to a similar extent between the wild type and *Scmh1*$^{-/-}$ (Fig. 5Bd). In contrast, the frequency of late pachytene spermatocytes, in which trimethylated H3-K27 was excluded, was significantly reduced in *Scmh1*$^{-/-}$ testes compared to wild type (Fig. 5Bd). This suggests that Scmh1 is required to maintain the exclusion of trimethylated H3-K27 from the XY body in late pachytene spermatocytes but not in early pachytene.

We went on to examine the localization of monomethylated histone H3 at K4 (H3-K4) and dimethylated histone H4 at K20 (H4-K20) because the mbt repeats, which are also found in the Scmh1 N-terminal, have been shown to exhibit specific binding to mono- and dimethylated H3-K9, monomethylated H3-K4 and mono- and dimethylated H4-K20 (Kim et al., 2006; Klymenko et al., 2006). Neither hypermonomethylation of H3-K4 nor underdimethylation of H4-K20 at the XY body were significantly different between wild-type and *Scmh1*$^{-/-}$ spermatocytes (Fig. 5Ca,b). It is particularly noteworthy that H4-K20 underdimethylation at the XY body, which was exclusively seen in the late pachytene spermatocytes in wild type, was not affected in the mutants (Y.T., unpublished). Taken together, these results show that apoptotic elimination of late pachytene spermatocytes in *Scmh1*$^{-/-}$ testes is preceded by failure in hypermethylation of H3-K9, exclusion of phosphorylated RNA pol II and Prc1 components and undermethylation of H3-K27 at the XY body, whereas it is not accompanied by changes in H3-K9 acetylation or methylation of H3-K4 or H4-K20. These results support the idea that changes in chromatin modifications at the XY body of *Scmh1*$^{-/-}$ spermatocytes are not simply a consequence of apoptotic elimination of late pachytene spermatocytes. Instead, Scmh1 was suggested to play the regulatory role for the sequential changes in chromatin modifications of the XY body.

## *Phc2* mutation alleviates spermatogenic defects in *Scmh1*$^{-/-}$ spermatocytes

We postulated that Scmh1 functions via its direct interaction with Prc1 in pachytene spermatocytes, as Scmh1 has been identified as a constituent of Prc1 components because, in general, mutant interactions of *PcG* alleles have been shown to modify the respective phenotypes in mammals as well (Bel et al., 1998; Akasaka et al., 2001; Isono et al., 2005). We have generated *Scmh1;Phc2* double mutants (dko) as Phc2 protein binds to Scmh1 via its SPM domain and the homozygous mutants were viable and fertile (Isono et al., 2005) (Y.T., unpublished). dko mice were viable and born according to the principles of Mendelian inheritance, although some of them exhibited growth retardation (Y.T., unpublished). The fertility of ten normal-sized dko and *Scmh1*$^{-/-}$ males was tested by natural mating to approximately 10-week-old C57BL/6 females. Strikingly, all the dko males were fertile, whereas half the *Scmh1*$^{-/-}$ males were sterile (Fig. 6B). Histological inspections revealed that all the dko testes were morphologically indistinguishable from wild type at day 35 pp and the frequency of apoptotic outbursts in dko was significantly reduced in comparison with littermate *Scmh1*$^{-/-}$ testes (Fig. 6A,C). Significant restorations of late pachytene spermatocytes were also revealed by substaging spermatocytes using antibodies against di-

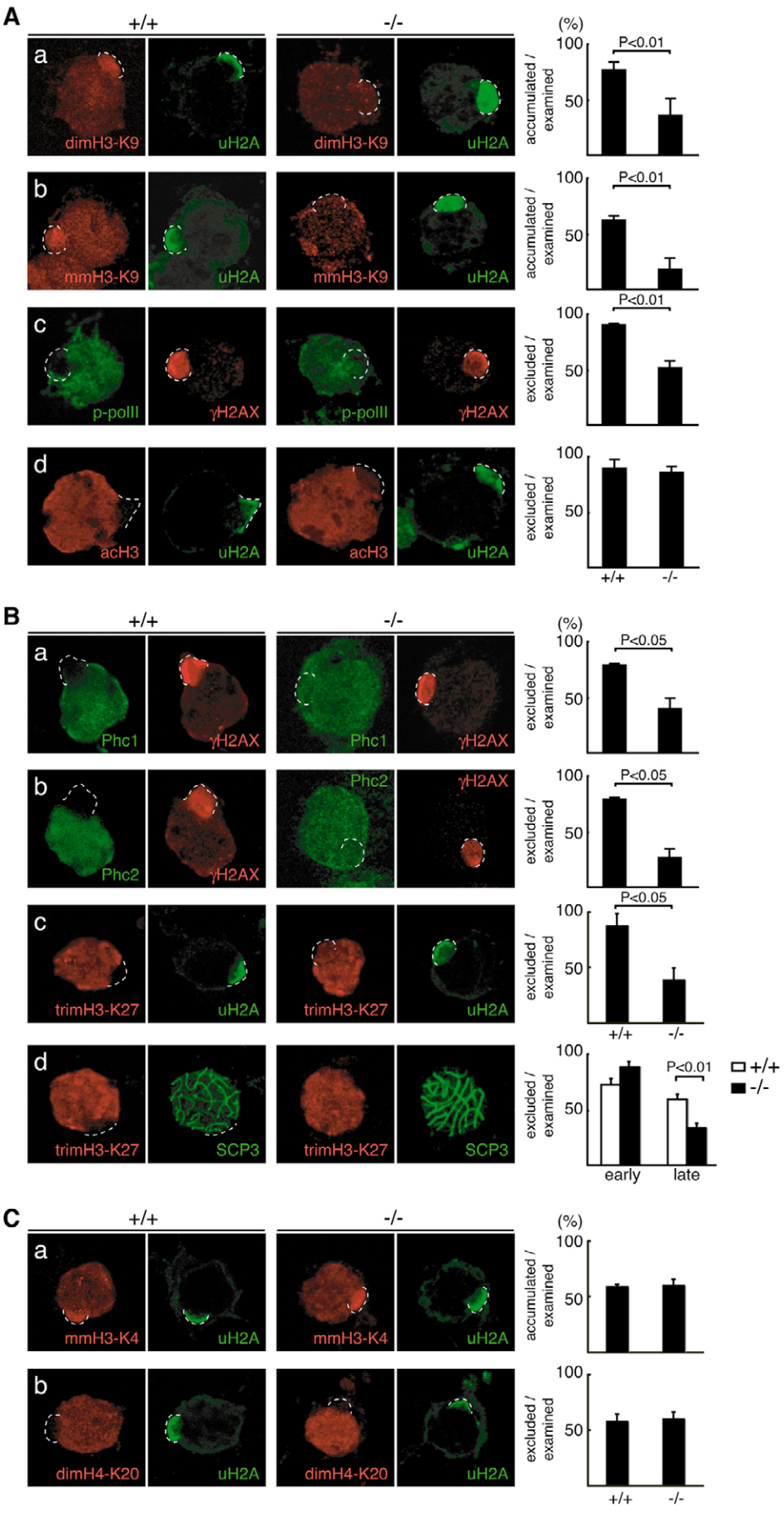


**Fig. 5. Altered chromatin modifications at the XY body in *Scmh1*$^{-/-}$ spermatocytes.**
(**A**) Immunostaining for dimethylated H3-K9, monomethylated H3-K9, phosphorylated RNA pol II, γH2A.X and uH2A in the spermatocyte spread. (**Aa**,**Ab**) Frequency of spermatocytes, in which dimethylated (a) or monomethylated (b) H3-K9 was enriched at the XY body demarcated by uH2A accumulation, was compared (left) and results were summarized (right). (**Ac**,**Ad**) Frequency of spermatocytes, in which phosphorylated RNA pol II (c) or acetylated H3-K9 (d) were excluded from the XY body, was compared (left) and results were summarized (right). (**Ba**,**Bb**) Frequency of spermatocytes, in which Phc1 (a) or Phc2 (b) were excluded from the XY body, was compared (left) and results were summarized (right). (**Bc**,**Bd**) Frequency of spermatocytes, in which trimethylated H3-K27 were excluded from the XY body was compared. Scp3 was used to substage the spermatocytes. (**C**) Frequency of spermatocytes, in which monomethylated H3-K4 (**Ca**) and dimethylated H4-K20 (**Cb**) were accumulated on the XY body, was compared (left) and results were summarized (right).

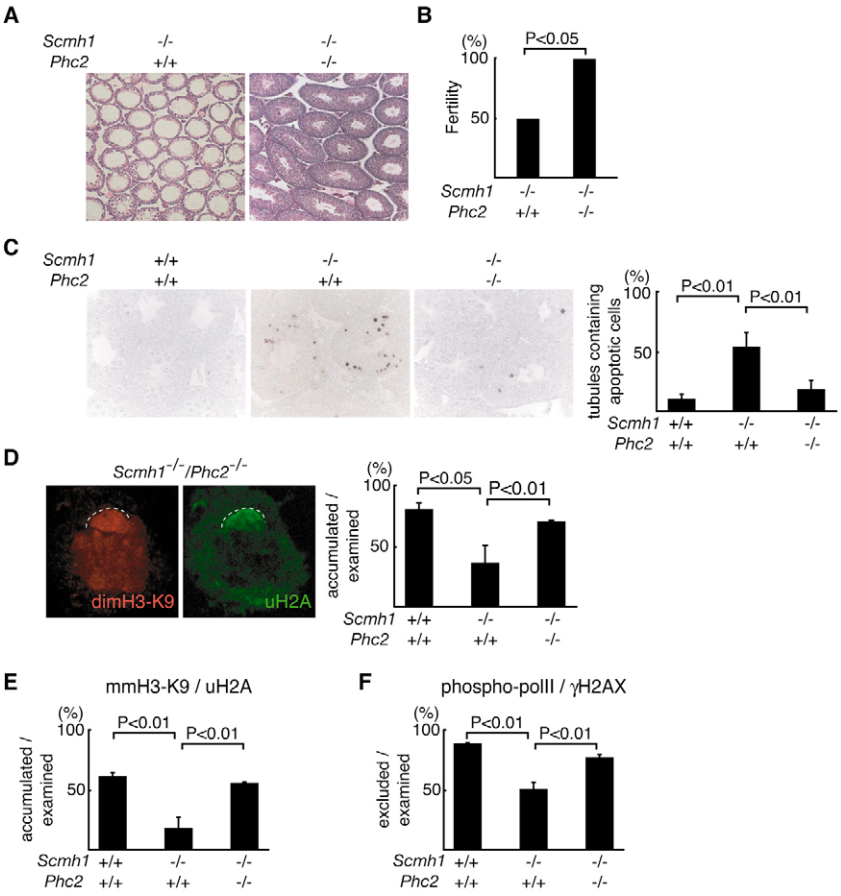


**Fig. 6. Restoration of spermatogenic defects in *Scmh1*$^{-/-}$ testes by *Phc2* mutation.** (**A**) Restoration of morphological defects in *Scmh1*$^{-/-}$ testes by *Phc2* mutation. (**B**) Restoration of fertility in *Scmh1*$^{-/-}$;*Phc2*$^{-/-}$ mice. Results from ten mice with respective genotypes were summarized. (**C**) Significant reduction of apoptotic outbursts in *Scmh1*$^{-/-}$;*Phc2*$^{-/-}$ testes compared with *Scmh1*$^{-/-}$ single mutants. (Left) Incidence of apoptosis was examined in wild-type, *Scmh1*$^{-/-}$ and *Scmh1*$^{-/-}$;*Phc2*$^{-/-}$ testes at day 19 pp by TUNEL staining. (Right) Three hundred seminiferous tubules derived from five mice with respective genotypes were analyzed for the presence of TUNEL-positive cells and the results were summarized. (**D**) Restoration of spermatocytes, in which dimethylated H3-K9 was enriched at the XY body in *Scmh1*$^{-/-}$;*Phc2*$^{-/-}$ testes (left). Frequency of spermatocytes, in which dimethylated H3-K9 was accumulated on the XY body, was summarized (right). (**E**,**F**) Frequency of spermatocytes, in which monomethylated H3-K9 was enriched at (E) and phosphorylated pol II was excluded from (F) the XY body in *Scmh1*$^{-/-}$;*Phc2*$^{-/-}$ testes was compared.

and monomethylated H3-K9, the phosphorylated form of RNA pol II and Phc1 (Fig. 6D-F and Y.T., unpublished). Defects in spermatogenesis were also significantly alleviated in *Scmh1*$^{-/-}$*Phc2*$^{+/-}$ albeit to a lesser extent than dkos (Y.T., unpublished). Therefore *Phc2* mutation coincidentally restored aberrant chromatin modifications seen in the XY body of *Scmh1*$^{-/-}$ spermatocytes and their developmental arrest at the late pachytene stage. Taken together, this evidence suggests that Scmh1 is a regulatory component of Prc1 that mediates exclusion of Prc1 from the XY body at the pachytene stage of meiosis. It is likely that the lack of Phc2 components may accelerate this exclusion irrespective of Scmh1.

## MSCI is not affected in *Scmh1*$^{-/-}$ spermatocytes

Transcriptional inactivation of sex chromosomes during spermatogenesis is accompanied by sequential changes in their histone modifications, which are notably affected in *Scmh1*$^{-/-}$ spermatocytes. We thus examined the degree of MSCI in *Scmh1*$^{-/-}$ testes, by performing genome-wide microarray-based analysis from three independent preparations of wild-type and *Scmh1*$^{-/-}$ spermatocytes at days 15, 18 and 20 pp and Cot1 RNA fluorescence in situ hybridization (FISH) (Fernandez-Capetillo et al., 2003; Turner et al., 2004; Turner et al., 2005). Average expression levels of genes located on the autosomes and sex chromosomes were compared between the wild type and *Scmh1*$^{-/-}$ after conventional normalization. No significant changes were found in the expression of autosomal and sex chromosomal genes in *Scmh1*$^{-/-}$ spermatocytes (see Fig. S5A in the supplementary material). Concordant with this result, the XY chromatin domain enriched in γH2A.X was negative for Cot-1 RNA in *Scmh1*$^{-/-}$ spermatocytes as well as the wild type (see Fig. S5B in the supplementary material). In conclusion, sequential chromatin modifications mediated by Scmh1 are not required to maintain MSCI.

## DISCUSSION

In this study, we generated *Scmh1* mutant mice and identified Scmh1 as an indispensable component of Prc1, based on the axial homeosis and premature senescence of MEFs in the homozygous mutants. We have further identified the role of Scmh1 in mediating the survival of late pachytene spermatocytes. Apoptotic elimination of *Scmh1*$^{-/-}$ spermatocytes is accompanied by the preceding failure of several specific chromatin modifications at the XY body, whereas synapsis of homologous autosomes is not affected. Therefore, it is suggested that Scmh1 is involved in regulating the sequential changes in chromatin modifications at the XY chromatin domain of the pachytene spermatocytes but is not required to maintain MSCI. Restoration of defects in *Scmh1*$^{-/-}$ spermatocytes by *Phc2* mutation indicates that Scmh1 exerts its molecular functions via its interaction with Prc1. Therefore, for the first time, we have been able to indicate a functional involvement of Prc1 during the meiotic prophase of male germ cells and a regulatory role of Scmh1 for Prc1, which presumably involves sex chromosomes.

Based on the present observations, we postulate that Scmh1 could primarily promote the exclusion of Prc1 components from the XY body in the pachytene spermatocytes because Scmh1 itself is a functional component of Prc1. By contrast, failure to maintain exclusion of trimethylated H3-K27 and to undergo H3-K9 methylation at the XY body in *Scmh1*$^{-/-}$ spermatocytes may occur

secondarily to the failure to exclude Prc1 from the XY body. At many loci, epistatic engagement of Prc1 by Prc2 has been shown to be essential for the mediation of transcriptional repression (Lee et al., 2006; Boyer et al., 2006; Fujimura et al., 2006). Preceding exclusion of trimethylated H3-K27, which represents Prc2 actions, for Prc1 exclusion from the XY body, is consistent with epistatic roles of Prc2 for Prc1 at the XY body. Therefore, Scmh1 may affect H3-K27 trimethylation at the XY body through the Prc1-Prc2 engagement. It is noteworthy that H3-K27 trimethylation has been shown to be regulated by Prc1 at the XY body. This may imply that Prc1-Prc2 engagement is a reciprocal rather than epistatic process at the XY body. This possibility should be addressed by using conditional mutants for Prc2 components. We also hypothesize a functional correlation between Prc1 exclusion and H3-K9 methylations at the XY body because the indispensable H3-K9 methyltransferase complex, composed of G9a and GLP, is constitutively associated with E2F6 complexes, which share at least Rnf2 and Ring1 components with Prc1. Moreover, several components of respective complexes are structurally related to each other (Ogawa et al., 2002; Trimarchi et al., 2001). Intriguingly, although Prc1 components, apart from Rnf2, have been shown to be excluded from the XY body at late pachytene stage, components of E2F6 complexes including Rnf2, RYBP, HP1γ and G9a are retained (Y.T., K.I. and H.K., unpublished). The most attractive scenario would be that exclusion of Prc1 is a prerequisite for the functional manifestation of E2F6 complexes to mediate the hypermethylation of H3-K9 at the XY body. We thus propose that Scmh1-mediated exclusion of Prc1 from the XY body might be a prerequisite for maintaining appropriate chromatin structure to undergo subsequent sequential chromatin remodeling of the XY chromatin in pachytene spermatocytes.

We also suggest that sequential changes in chromatin modifications of the sex chromosomes in the pachytene spermatocytes might be monitored by some meiotic checkpoint mechanisms. This is supported by the temporal concurrence of Prc1 exclusion from the XY body and apoptotic depletion of meiotic spermatocytes, their coincidental restorations by *Phc2* mutation, and normal oogenesis and fertility in *Scmh1*$^{-/-}$ females (Y.T. and H.K., unpublished). In addition, defects in the XY body formations have been shown to correlate with apoptotic depletion of meiotic spermatocytes by studies using *H2A.X* and *Brca1* mutants, although developmental arrests occurred by early pachytene stage (Fernandez-Capetillo et al., 2003; Xu et al., 2003). However, this link has not been substantially demonstrated.

Although Scmh1 has been shown to act together with Prc1, the role of Scmh1 for Prc1 might be modified in a tissue- or locus-specific manner because spermatogenic defects by *Scmh1* mutation are restored by *Phc2* mutation, whereas premature senescence of MEFs is enhanced mutually by both mutations (Y.T. and H.K., unpublished). This is supported by an immunofluorescence study revealing the co-localization of Scmh1 with other class 2 PcG proteins in subnuclear speckles in U2OS cells, whereas in female trophoblastic stem (TS) cells it is excluded from the inactive X chromosome domain, which is intensely decorated by Rnf2, Phc2 and Rnf110 (see Fig. S6A,B in the supplementary material) (Plath et al., 2004; de Napoles et al., 2004). It may be possible to postulate some additional factors that modify the molecular functions or subnuclear localization of Scmh1. Indeed, most of the soluble pool of SCM in *Drosophila* embryos is not stably associated with Prc1, although SCM is capable of assembling with the Polyhomeotic protein by their respective SPM domains in the Polycomb core complex (Peterson et al., 2004). As the SPM domain is shared, not only by *polyhomeotic* homologs, but also by multiple paralogs of the *Drosophila Scm* gene, namely *Scml1*, *Scml2*, *Sfmbt*, *l(3)mbt3* and others in mammals, these structurally related gene products may potentially interact with Scmh1 and modulate its functions. Conservations of crucial amino acid residues required for the mutual interaction of SPM domains and multiple mbt repeats in these proteins may further suggest functional overlap with Scmh1. It is notable that phenotypic expressions of *Scmh1* mutation are quite variable during spermatogenesis and axial development even after more than five times backcrossing to a C57Bl/6 background. This incomplete penetrance might involve multiple paralogs of the canonical Scm proteins, which may act in compensatory manner for *Scmh1* mutation, as revealed between *Rnf110* and *Bmi1* or *Phc1* and *Phc2* (Akasaka et al., 2001; Isono et al., 2005).

We are grateful to Drs M. Vidal and W. Baarends for the critical reading of the manuscript. This project was supported by Special Coordination Funds for Promoting Science and Technology from the Ministry of Education, Culture, Sports, Science and Technology, the Japanese Government.

**Supplementary material**

Supplementary material for this article is available at http://dev.biologists.org/cgi/content/full/134/3/579/DC1

**References**

**Akasaka, T., Kanno, M., Balling, R., Mieza, M. A., Taniguchi, M. and Koseki, H.** (1996). A role for mel-18, a Polycomb group-related vertebrate gene, during the anteroposterior specification of the axial skeleton. *Development* **122**, 1513-1522.

**Akasaka, T., van Lohuizen, M., van der Lugt, N., Mizutani-Koseki, Y., Kanno, M., Taniguchi, M., Vidal, M., Alkema, M., Berns, A. and Koseki, H.** (2001). Mice doubly deficient for the Polycomb Group genes Mel18 and Bmi1 reveal synergy and requirement for maintenance but not initiation of Hox gene expression. *Development* **128**, 1587-1597.

**Atsuta, T., Fujimura, S., Moriya, H., Vidal, M., Akasaka, T. and Koseki, H.** (2001). Production of monoclonal antibodies against mammalian Ring1B proteins. *Hybridoma* **20**, 43-46.

**Baarends, W. M., Hoogerbrugge, J. W., Roest, H. P., Ooms, M., Vreeburg, J., Hoeijmakers, J. H. and Grootegoed, J. A.** (1999). Histone ubiquitination and chromatin remodeling in mouse spermatogenesis. *Dev. Biol.* **207**, 322-333.

**Baarends, W. M., Wassenaar, E., van der Laan, R., Hoogerbrugge, J., Sleddens-Linkels, E., Hoeijmakers, J. H., de Boer, P. and Grootegoed, J. A.** (2005). Silencing of unpaired chromatin and histone H2A ubiquitination in mammalian meiosis. *Mol. Cell. Biol.* **25**, 1041-1053.

**Bel, S., Core, N., Djabali, M., Kieboom, K., Van der Lugt, N., Alkema, M. J. and Van Lohuizen, M.** (1998). Genetic interactions and dosage effects of Polycomb group genes in mice. *Development* **125**, 3543-3551.

**Bornemann, D., Miller, E. and Simon, J.** (1996). The Drosophila Polycomb group gene Sex comb on midleg (Scm) encodes a zinc finger protein with similarity to polyhomeotic protein. *Development* **122**, 1621-1630.

**Boyer, L. A., Plath, K., Zeitlinger, J., Brambrink, T., Mederios, L. A., Lee, T. I., Levine, S. S., Wernig, M., Tajonar, A., Ray, M. K. et al.** (2006). Polycomb complexes repress developmental regulators in murine embryonic stem cells. *Nature* **441**, 349-353.

**Cao, R., Wang, L., Xia, L., Erdjument-Bromage, H., Tempst, P. and Zhang, Y.** (2002). Role of histone H3 lysine 27 methylation in Polycomb-group silencing. *Science* **298**, 1039-1043.

**Celeste, A., Petersen, S., Romanienko, P. J., Fernandez-Capetillo, O., Chen, H. T., Sedelnikova, O. A., Reina-San-Martin, B., Coppola, V., Meffre, E., Difilippantonio, M. J. et al.** (2002). Genomic instability in mice lacking histone H2AX. *Science* **296**, 922-927.

**Cohen, P. E. and Pollard, J. W.** (2001). Regulation of meiotic recombination and prophase I progression in mammals. *BioEssays* **23**, 996-1009.

**de Napoles, M., Mermoud, J. E., Wakao, R., Tang, Y. A., Endoh, M., Appanah, R., Nesterova, T. B., Silva, J., Otte, A. P., Vidal, M. et al.** (2004). Polycomb group proteins Ring1A/B link ubiquitylation of histone H2A to heritable gene silencing and X inactivation. *Dev. Cell* **7**, 663-676.

**Fernandez-Capetillo, O., Mahadevaiah, S. K., Celeste, A., Romanienko, P. J., Camerini-Otero, R. D., Bonner, W. M., Manova, K., Burgoyne, P. and Nussenzweig, A.** (2003). H2AX is required for chromatin remodeling and inactivation of sex chromosomes in male mouse meiosis. *Dev. Cell* **4**, 497-508.

**Foulkes, N. S., Mellstrom, B., Benusiglio, E. and Sassone-Corsi, P.** (1992). Developmental switch of CREM function during spermatogenesis: from antagonist to activator. *Nature* **355**, 80-84.

**Franke, A., DeCamillis, M., Zink, D., Cheng, N., Brock, H. W. and Paro, R.**

(1992). Polycomb and polyhomeotic are constituents of a multimeric protein complex in chromatin of Drosophila melanogaster. *EMBO J.* **11**, 2941-2950.
**Fujimura, Y., Isono, K., Vidal, M., Endoh, M., Kajita, H., Mizutani-Koseki, Y., Takihara, Y., Van Lohuizen, M., Otte, A. P., Jenuwein, T. et al.** (2006). Distinct roles of Polycomb group gene products in transcriptionally repressed and active domains of *Hoxb*8. *Development* **133**, 2371-2381.
**Fujiwara, Y., Komiya, T., Kawabata, H., Sato, M., Fujimoto, H., Furusawa, M. and Noce, T.** (1994). Isolation of a DEAD-family protein gene that encodes a murine homolog of Drosophila vasa and its specific expression in germ cell lineage. *Proc. Natl. Acad. Sci. USA* **91**, 12258-12262.
**Gebuhr, T. C., Bultman, S. J. and Magnuson, T.** (2000). Pc-G/trx-G and the SWI/SNF connection: developmental gene regulation through chromatin remodeling. *Genesis* **26**, 189-197.
**Habu, T., Taki, T., West, A., Nishimune, Y. and Morita, T.** (1996). The mouse and human homologs of DMC1, the yeast meiosis-specific homologous recombination gene, have a common unique form of exon-skipped transcript in meiosis. *Nucleic Acids Res.* **24**, 470-477.
**Hoyer-Fender, S., Costanzi, C. and Pehrson, J. R.** (2000). Histone macroH2A1.2 is concentrated in the XY-body by the early pachytene stage of spermatogenesis. *Exp. Cell Res.* **258**, 254-260.
**Isono, K., Fujimura, Y., Shinga, J., Yamaki, M. O., Wang, J., Takihara, Y., Murahashi, Y., Takada, Y., Mizutani-Koseki, Y. and Koseki, H.** (2005). Mammalian polyhomeotic homologues Phc2 and Phc1 act in synergy to mediate polycomb repression of Hox genes. *Mol. Cell. Biol.* **25**, 6694-6706.
**Jacobs, J. J., Kieboom, K., Marino, S., DePinho, R. A. and van Lohuizen, M.** (1999). The oncogene and Polycomb-group gene bmi-1 regulates cell proliferation and senescence through the ink4a locus. *Nature* **397**, 164-168.
**Jürgens, G.** (1985). A group of genes controlling spatial expression of the bithorax complex in *Drosophila*. *Nature* **316**, 153-155.
**Kamijo, T., Zindy, F., Roussel, M. F., Quelle, D. E., Downing, J. R., Ashmun, R. A., Grosveld, G. and Sherr, C. J.** (1997). Tumor suppression at the mouse INK4a locus mediated by the alternative reading frame product p19ARF. *Cell* **91**, 649-659.
**Kessel, M. and Gruss, P.** (1991). Homeotic transformations of murine vertebrae and concomitant alteration of Hox codes induced by retinoic acid. *Cell* **67**, 89-104.
**Khalil, A. M., Boyar, F. Z. and Driscoll, D. J.** (2004). Dynamic histone modifications mark sex chromosome inactivation and reactivation during mammalian spermatogenesis. *Proc. Natl. Acad. Sci. USA* **101**, 16583-16587.
**Kim, J., Daniel, J., Espejo, A., Lake, A., Krishna, M., Xia, L., Zhang, Y. and Bedford, M. T.** (2006). Tudor, MBT and chromo domains gauge the degree of lysine methylation. *EMBO Rep.* **7**, 397-403.
**Klink, A., Lee, M. and Cooke, H. J.** (1997). The mouse synaptosomal complex protein gene Sycp3 maps to band C of chromosome 10. *Mamm. Genome* **8**, 376-377.
**Klymenko, T., Papp, B., Fischle, W., Köcher, T., Schelder, M., Fritsch, C., Wild, B., Wilm, M. and Müller, J.** (2006). A Polycomb group protein complex with sequence-specific DNA-binding and selective methyl-lysine-binding activities. *Genes Dev.* **20**, 1110-1122.
**Kuzmichev, A., Nishioka, K., Erdjument-Bromage, H., Tempst, P. and Reinberg, D.** (2002). Histone methyltransferase activity associated with a human multiprotein complex containing the Enhancer of Zeste protein. *Genes Dev.* **16**, 2893-2905.
**Laible, G., Wolf, A., Dorn, R., Reuter, G., Nislow, C., Lebersorger, A., Popkin, D., Pillus, L. and Jenuwein, T.** (1997). Mammalian homologues of the Polycomb-group gene Enhancer of zeste mediate gene silencing in Drosophila heterochromatin and at S. cerevisiae telomeres. *EMBO J.* **16**, 3219-3232.
**Lee, T. I., Jenner, R. G., Boyer, L. A., Guenther, M. G., Levine, S. S., Kumar, R. M., Chevalier, B., Johnstone, S. E., Cole, M. F., Isono, K. et al.** (2006). Control of developmental regulators by Polycomb in human embryonic stem cells. *Cell* **125**, 301-313.
**Levine, S. S., Weiss, A., Erdjument-Bromage, H., Shao, Z., Tempst, P. and Kingston, R. E.** (2002). The core of the polycomb repressive complex is compositionally and functionally conserved in flies and humans. *Mol. Cell. Biol.* **22**, 6070-6078.
**Mahadevaiah, S. K., Turner, J. M., Baudat, F., Rogakou, E. P., de Boer, P., Blanco-Rodriguez, J., Jasin, M., Keeney, S., Bonner, W. M. and Burgoyne, P. S.** (2001). Recombinational DNA double-strand breaks in mice precede synapsis. *Nat. Genet.* **27**, 271-276.
**Mettus, R. V., Litvin, J., Wali, A., Toscani, A., Latham, K., Hatton, K. and Reddy, E. P.** (1994). Murine A-myb: evidence for differential splicing and tissue-specific expression. *Oncogene* **9**, 3077-3086.
**Miyagishima, H., Isono, K., Fujimura, Y., Iyo, Y., Takihara, Y., Masumoto, H., Vidal, M. and Koseki, H.** (2003). Dissociation of mammalian Polycomb-group proteins, Ring1B and Rae28/Ph1, from the chromatin correlates with configuration changes of the chromatin in mitotic and meiotic prophase. *Histochem. Cell Biol.* **120**, 111-119.
**Montini, E., Buchner, G., Spalluto, C., Andolfi, G., Caruso, A., den Dunnen, J. T., Trump, D., Rocchi, M., Ballabio, A. and Franco, B.** (1999). Identification of SCML2, a second human gene homologous to the Drosophila sex comb on midleg (Scm): a new gene cluster on Xp22. *Genomics* **58**, 65-72.
**Odorisio, T., Mahadevaiah, S. K., McCarrey, J. R. and Burgoyne, P. S.** (1996). Transcriptional analysis of the candidate spermatogenesis gene Ube1y and of the closely related Ube1x shows that they are coexpressed in spermatogonia and spermatids but are repressed in pachytene spermatocytes. *Dev. Biol.* **180**, 336-343.
**Ogawa, H., Ishiguro, K., Gaubatz, S., Livingston, D. M. and Nakatani, Y.** (2002). A complex with chromatin modifiers that occupies E2F- and Myc-responsive genes in G0 cells. *Science* **296**, 1132-1136.
**Paro, R.** (1995). Propagating memory of transcriptional states. *Trends Genet.* **11**, 295-297.
**Perry, J., Palmer, S., Gabriel, A. and Ashworth, A.** (2001). A short pseudoautosomal region in laboratory mice. *Genome Res.* **11**, 1826-1832.
**Peterson, A. J., Mallin, D. R., Francis, N. J., Ketel, C. S., Stamm, J., Voeller, R. K., Kingston, R. E. and Simon, J. A.** (2004). Requirement for sex comb on midleg protein interactions in Drosophila polycomb group repression. *Genetics* **167**, 1225-1239.
**Pirrotta, V.** (1997). PcG complexes and chromatin silencing. *Curr. Opin. Genet. Dev.* **7**, 249-258.
**Plath, K., Talbot, D., Hamer, K. M., Otte, A. P., Yang, T. P., Jaenisch, R. and Panning, B.** (2004). Developmentally regulated alterations in Polycomb repressive complex 1 proteins on the inactive X chromosome. *J. Cell Biol.* **167**, 1025-1035.
**Richler, C., Dhara, S. K. and Wahrman, J.** (2000). Histone macroH2A1.2 is concentrated in the XY compartment of mammalian male meiotic nuclei. *Cytogenet. Cell Genet.* **89**, 118-120.
**Scherthan, H., Jerratsch, M., Dhar, S., Wang Y. A., Goff, S. P. and Pandita T. K.** (2000). Meiotic telomere distribution and Sertoli cell nuclear architecture are altered in Atm- and Atm-p53-deficient mice. *Mol. Cell Biol.* **20**, 7773-7783.
**Schumacher, A., Faust, C. and Magnuson, T.** (1996). Positional cloning of a global regulator of anterior-posterior patterning in mice. *Nature* **384**, 648.
**Sewalt, R. G., van der Vlag, J., Gunster, M. J., Hamer, K. M., den Blaauwen, J. L., Satijn, D. P., Hendrix, T., van Driel, R. and Otte, A. P.** (1998). Characterization of interactions between the mammalian polycomb-group proteins Enx1/EZH2 and EED suggests the existence of different mammalian polycomb-group protein complexes. *Mol. Cell. Biol.* **18**, 3586-3595.
**Shao, Z., Raible, F., Mollaaghababa, R., Guyon, J. R., Wu, C. T., Bender, W. and Kingston, R. E.** (1999). Stabilization of chromatin structure by PRC1, a Polycomb complex. *Cell* **98**, 37-46.
**Singer-Sam, J., Robinson, M. O., Bellve, A. R., Simon, M. I. and Riggs, A. D.** (1990). Measurement by quantitative PCR of changes in HPRT, PGK-1, PGK-2, APRT, MTase, and Zfy gene transcripts during mouse spermatogenesis. *Nucleic Acids Res.* **18**, 1255-1259.
**Strahl, B. D. and Allis, C. D.** (2000). The language of covalent histone modifications. *Nature* **403**, 41-45.
**Sweeney, C., Murphy, M., Kubelka, M., Ravnik, S. E., Hawkins, C. F., Wolgemuth, D. J. and Carrington, M.** (1996). A distinct cyclin A is expressed in germ cells in the mouse. *Development* **122**, 53-64.
**Tanaka, S. S., Toyooka, Y., Akasu, R., Katoh-Fukui, Y., Nakahara, Y., Suzuki, R., Yokoyama, M. and Noce, T.** (2000). The mouse homolog of Drosophila Vasa is required for the development of male germ cells. *Genes Dev.* **14**, 841-853.
**Tomotsune, D., Takihara, Y., Berger, J., Duhl, D., Joo, S., Kyba, M., Shirai, M., Ohta, H., Matsuda, Y., Honda, B. M. et al.** (1999). A novel member of murine Polycomb-group proteins, Sex comb on midleg homolog protein, is highly conserved, and interacts with RAE28/mph1 in vitro. *Differentiation* **65**, 229-239.
**Trimarchi, J. M., Fairchild, B., Wen, J. and Lees, J. A.** (2001). The E2F6 transcription factor is a component of the mammalian Bmi1-containing polycomb complex. *Proc. Natl. Acad. Sci. USA* **98**, 1519-1524.
**Turner, J. M., Mahadevaiah, S. K., Benavente, R., Offenberg, H. H., Heyting, C. and Burgoyne, P. S.** (2000). Analysis of male meiotic "sex body" proteins during XY female meiosis provides new insights into their functions. *Chromosoma* **109**, 426-432.
**Turner, J. M., Burgoyne, P. S. and Singh, P. B.** (2001). M31 and macroH2A1.2 colocalize at the pseudoautosomal region during mouse meiosis. *J. Cell Sci.* **114**, 3367-3375.
**Turner, J. M., Aprelikova, O., Xu, X., Wang, R., Kim, S., Chandramouli, G. V., Barrett, J. C., Burgoyne, P. S. and Deng, C. X.** (2004). BRCA1, histone H2AX phosphorylation, and male meiotic sex chromosome inactivation. *Curr. Biol.* **14**, 2135-2142.
**Turner, J. M., Mahadevaiah, S. K., Fernandez-Capetillo, O., Nussenzweig, A., Xu, X., Deng, C. X. and Burgoyne, P. S.** (2005). Silencing of unsynapsed meiotic chromosomes in the mouse. *Nat. Genet.* **37**, 41-47.
**Usui, H., Ichikawa, T., Kobayashi, K. and Kumanishi, T.** (2000). Cloning of a novel murine gene Sfmbt, Scm-related gene containing four mbt domains, structurally belonging to the Polycomb group of genes. *Gene* **248**, 127-135.
**van de Vosse, E., Walpole, S. M., Nicolaou, A., van der Bent, P., Cahn, A., Vaudin, M., Ross, M. T., Durham, J., Pavitt, R., Wilkinson, J. et al.** (1998). Characterization of SCML1, a new gene in Xp22, with homology to developmental polycomb genes. *Genomics* **49**, 96-102.

**van der Vlag, J. and Otte, A. P.** (1999). Transcriptional repression mediated by the human polycomb-group protein EED involves histone deacetylation. *Nat. Genet.* **23**, 474-478.
**van Lohuizen, M., Tijms, M., Voncken, J. W., Schumacher, A., Magnuson, T. and Wientjens, E.** (1998). Interaction of mouse polycomb-group (Pc-G) proteins Enx1 and Enx2 with Eed: indication for separate Pc-G complexes. *Mol. Cell. Biol.* **18**, 3572-3579.
**Wang, H., Wang, L., Erdjument-Bromage, H., Vidal, M., Tempst, P., Jones, R. S. and Zhang, Y.** (2004). Role of histone H2A ubiquitination in Polycomb silencing. *Nature* **431**, 873-878.
**Watanabe, D., Yamada, K., Nishina, Y., Tajima, Y., Koshimizu, U., Nagata, A. and Nishimune, Y.** (1994). Molecular cloning of a novel Ca(2+)-binding protein (calmegin) specifically expressed during male meiotic germ cell development. *J. Biol. Chem.* **269**, 7744-7749.
**Xu, X., Aprelikova, O., Moens, P., Deng, C. X. and Furth, P. A.** (2003). Impaired meiotic DNA-damage repair and lack of crossing-over during spermatogenesis in BRCA1 full-length isoform deficient mice. *Development* **130**, 2001-2012.
**Yuasa, S.** (1996). Bergmann glial development in the mouse cerebellum as revealed by tenascin expression. *Anat. Embryol.* **194**, 223-234.
**Zhao, G. Q. and Hogan, B. L.** (1996). Evidence that mouse Bmp8a (Op2) and Bmp8b are duplicated genes that play a role in spermatogenesis and placental development. *Mech. Dev.* **57**, 159-168.